

# LCS Graph Kernel Based on Wasserstein Distance in Longest Common Subsequence Metric Space

Jianming Huang <sup>\*</sup>      Zhongxi Fang <sup>†</sup>      Hiroyuki Kasai <sup>‡§</sup>

December 8, 2020

## Abstract

For graph classification tasks, many methods use a common strategy to aggregate information of vertex neighbors. Although this strategy provides an efficient means of extracting graph topological features, it brings excessive amounts of information that might greatly reduce its accuracy when dealing with large-scale neighborhoods. Learning graphs using paths or walks will not suffer from this difficulty, but many have low utilization of each path or walk, which might engender information loss and high computational costs. To solve this, we propose a graph kernel using a longest common subsequence (LCS kernel) to compute more comprehensive similarity between paths and walks, which resolves substructure isomorphism difficulties. We also combine it with optimal transport theory to extract more in-depth features of graphs. Furthermore, we propose an LCS metric space and apply an adjacent point merge operation to reduce its computational costs. Finally, we demonstrate that our proposed method outperforms many state-of-the-art graph kernel methods.

## 1 Introduction

Graph-structured data have been used widely in various fields, such as chemoinformatics, bioinformatics, social networks, and computer vision [1, 2]. In graph-structured data classification tasks, a key difficulty is finding a criterion with which to compare graphs. However, no matter what method is used for comparison, graph isomorphism is a common difficulty that must be confronted and overcome: Do two graphs have identical topology? The degree to which two graphs mutually fit is usually regarded as similarity between two graphs. However, graph isomorphism has not been proved as NP complete. To date, no polynomial-time solution has been reported [3].

### 1.1 Breadth-first strategy and Depth-first strategy

Various strategies are available to assess graph isomorphism. Some studies specifically find a relation between vertices and their neighbors. This type of strategy is a *breadth-first strategy*, which tends to

---

<sup>\*</sup>Dept. of Computer Science and Communications Eng, Graduate School of Fundamental Science and Engineering, WASEDA University, 3-4-1 Okubo, Shinjuku-ku, Tokyo 169-8555, Japan (e-mail: koukenmei@toki.waseda.jp)

<sup>†</sup>Dept. of Computer Science and Eng., School of Fundamental Science and Eng., WASEDA University, 3-4-1 Okubo, Shinjuku-ku, Tokyo 169-8555, Japan (e-mail: fzx@akane.waseda.jp)

<sup>‡</sup>Dept. of Communications and Computer Eng. & Dept. of Computer Science and Eng., WASEDA University, 3-4-1 Okubo, Shinjuku-ku, Tokyo 169-8555, Japan (e-mail: hiroyuki.kasai@waseda.jp)

<sup>§</sup>H. Kasai was partially supported by JSPS KAKENHI Grant Numbers JP16K00031 and JP17H01732, and by Support Center for Advanced Telecomm. Technology Research (SCAT).

construct a neighbor network surrounding a certain vertex. As immediate instances, the Weisfeiler–Lehman graph kernel [4] uses the theory of the Weisfeiler–Lehman test [5], where vertex neighbors are aggregated as a new vertex label using a hash mapping function. The new label denotes a certain neighborhood pattern. Then graph isomorphism is resolved through comparison of these compressed labels of topological patterns. However, such breadth-first strategies entail several shortcomings. (1) Because breadth-first strategies are based on aggregating information of all neighbors, the embedding of a vertex usually involves excessive information, especially in a dense graph. (2) As the depth of a neighbor network increases, it grows geometrically, as does the quantity of information, especially when we want to assess the relationships of vertices that are mutually distant.

In other avenues of development, some studies have specifically examined paths and walks of graphs. In contrast to breadth-first strategies, they learn graph topology by comparing paths or walks. As immediate instances, one can find explanations of random walk graph kernel [6] and shortest path graph kernel [7] in the literature. We consider these as *depth-first strategies*, which use a simple form of subgraphs to learn the subgraph structure, instead of using complicatedly connected neighbor networks. In this manner, comparison of neighbor networks is transformed to a problem of comparing sets of path (or walks). It becomes easier to solve problems presented by breadth-first strategies. Nevertheless, path-based (or walk-based) methods are adversely affected by the common truth that they entail high computational costs because sampled paths (or walks) are usually numerous and have high redundancy.

## 1.2 Path comparing strategy

In path-based and walk-based methods, a traditional strategy to compare two path sequences is to judge if the two paths are completely identical. Taking the random walk kernel for example, two random walks are judged as common if their lengths are equal, and also if the label sequences are identical for labeled graphs. Other methods such as embedding-based methods assess the compared objects to ascertain if they have the same dimensions. However, these comparison strategies do not make full use of path sequences. Most of them do not consider subsequence similarity. However, these path sequences also entail a substructure isomorphism problem. In contrast to normal graph isomorphism, because of the special structures of paths, these isomorphism problems of paths are solvable in polynomial time using sequence comparison methods. Our proposed method leverages the *longest common subsequence* to solve path comparison problems.

### 1.2.1 Application of Optimal Transport (OT) theory

Because of computational improvements in solving optimal transport problems in recent years, optimal transport theory [8, 9] has been used in many machine-learning domains. Many studies have examined graph classification based on optimal transport theory. A representative product of those examinations is Wasserstein–Weisfeiler–Lehman Graph Kernels (WWL) [10], which improved the Weisfeiler–Lehman kernel by replacing a traditional  $\mathcal{R}$ -Convolution framework [11] with an optimal transport scheme. Most earlier graph kernel studies use the  $\mathcal{R}$ -Convolution framework, which tends to decompose a graph into several substructures such as subgraphs, paths, vertices, and edges; then the overall graph similarity is computed by aggregating similarity between substructures. However, traditional aggregating strategies such as sum, max, and min are too simple. They might be unable to capture complex features of graph structures. Our proposed method also uses optimal transport schemes to compute kernel values, but unlike WWL and other methods, we computed optimal transport over two sets of paths.

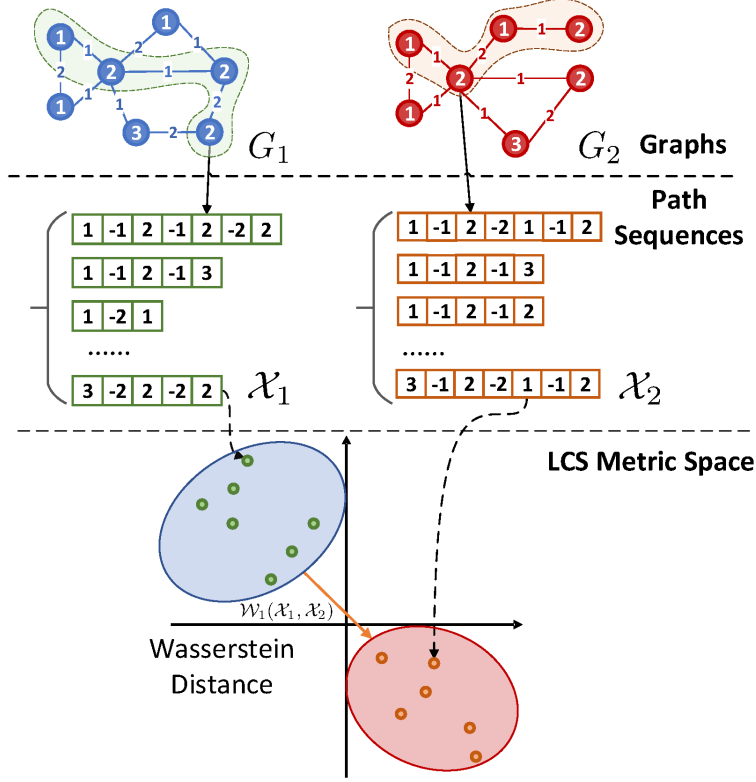


Figure 1: Visual summary of the LCS graph kernel. Shortest paths are serialized as label sequences and are mapped to an LCS metric space. The Wasserstein distance of two distributions in this space is used as the value of the LCS kernel.

### 1.2.2 Proposed method

To overcome shortcomings of breadth-first strategies, and to reduce high computational costs of current path-based methods, we propose path-comparison methods using the longest common sub-sequences (LCS) and optimal transport theory. We also apply this method to graph classification tasks, and present the LCS graph kernel. Figure 1 portrays a summary of the LCS graph kernel. In our method, we first perform shortest path serialization to transform all vertex-to-vertex shortest paths as path sequences; then we define a shortest path sequence set to represent the graph structure. We then map these path sequence sets to an LCS metric space, where a metric between two sequences is based on the length of their longest common subsequence. In the final step, we use the 1-Wasserstein distance of two distributions as our kernel value. We propose a basic method and a fast method. The former exhibits the basic concepts of our proposal. The latter is an improved version, which greatly reduces computational costs. Generally, our contributions can be summarized as described below.

- We present a method to compare labeled graphs using the longest common subsequence of path sequences and optimal transport theory, which transforms the graph isomorphism problem to a sequence comparison problem. It is also able to make full use of a single path sequence:
- We conduct numerical experiments on popular datasets, showing that our proposed method outperforms many state-of-the-art methods in graph classification tasks.

## 2 Preliminaries

This section first introduces some notation and preliminary points of graphs. Hereinafter, we represent scalars as lower-case letters ( $a, b, \dots$ ), vectors as bold typeface lower-case letters ( $\mathbf{a}, \mathbf{b}, \dots$ ), and matrices as bold typeface capitals ( $\mathbf{A}, \mathbf{B}, \dots$ ). An element at  $(i, j)$  of a matrix  $\mathbf{A}$  is represented as  $\mathbf{A}(i, j)$ .  $\mathbf{1}_n = (1, 1, \dots, 1)^T \in \mathbb{R}^n$ . We write  $\mathbb{R}_+^n$  to denote non-negative  $n$ -dimensional vector. Also,  $\mathbb{R}_+^{n \times m}$  represents a nonnegative matrix of size  $n \times m$ . The unit-simplex, simply called *simplex*, is denoted by  $\Delta_n$ , which is the subset of  $\mathbb{R}^n$  comprising all nonnegative vectors for which sums are 1. In addition,  $\delta_x$  is the Dirac function at  $x$ .

### 2.1 Preliminaries of graphs

A graph is a pair  $G = (\mathcal{V}, \mathcal{E})$  consisting of a set of  $n$  vertices (or nodes)  $\mathcal{V} = \{v_1, v_2, \dots, v_n\}$  and a set of  $m$  edges  $\mathcal{E} \subseteq \mathcal{V} \times \mathcal{V}$ .  $G$  is an undirected graph if a graph  $G$  includes only edges with no direction. The numbers of vertices and edges are, respectively,  $|\mathcal{V}|$  and  $|\mathcal{E}|$ . If two vertices, say  $v_i, v_j \in \mathcal{V}$ , are connected by an edge  $e$ , then this edge is denoted as  $e_{ij}$ . These two vertices are said to be adjacent or neighbors. We consider only undirected graphs with no self-loop.

Given an undirected graph  $G = (\mathcal{V}, \mathcal{E})$  and a vertex  $v_i \in \mathcal{V}$ , the degree of  $v_i$  in  $G$ , denoted as  $\sigma_i$ , is the number of edges incident to  $v_i$ . It is defined as  $\sigma_i = |\{v_j : e_{ij} \in \mathcal{E}\}| = |\mathcal{N}(v_i)|$ , where  $\mathcal{N}(v_i)$  represents the neighborhood set of  $v_i$ .

A walk in a graph  $G = (\mathcal{V}, \mathcal{E})$  is a sequence of vertices  $v_1, v_2, \dots, v_{k+1}$ , where  $v_i \in \mathcal{V}$  for all  $1 \leq i \leq k+1$  and  $v_i, v_{i+1} \in \mathcal{V}$  for all  $1 \leq i \leq k$ . The walk length is equal to the number of edges in the sequence, i.e.,  $k$  in the case above. A walk in which  $v_i \neq v_j \Leftrightarrow i \neq j$  is called a path. The path between the two adjacent vertices is equivalent to the edge. A set of paths between two non-adjacent vertices is denoted as  $\mathcal{P}_{i,j}$ . One path of  $\mathcal{P}_{i,j}$  is denoted as  $p_{i,j}$ . Moreover, the length of  $p_{i,j}$  is denoted as  $|p_{i,j}|$ . A shortest path, denoted as  $p_{i,j}^*$ , from vertex  $v_i$  to vertex  $v_j$  of a graph  $G$ , is a path from  $v_i$  to  $v_j$  such that no other path exists between these two vertices with smaller length.

### 2.2 Longest common subsequence

A sequence is defined mathematically as an enumerated collection of objects of a certain order, where repetition of elements is allowed. The length of a sequence denotes the number of its elements. Given a sequence with length  $n$ , it can be written as  $\mathbf{x} = (x_i)_{i=1}^n$ , where  $x_i$  denotes the  $i$ -th element. A subsequence of a given sequence is derived by removing some elements of the original sequence under the premise that the order of the remaining elements is retained as the original sequence. For example, given a sequence of  $(1, 2, 3, 4, 5)$ , both  $(2, 3, 4)$  and  $(1, 3, 5)$  are subsequences of the original sequence. The definition of the longest common subsequence problem can be presented as shown below [12, 13].

**Definition 1** (Longest Common Subsequence Problem). *The goal of a longest common subsequence problem is to find a sequence  $\mathbf{x}^*$  that satisfies the following conditions: (1)  $\mathbf{x}^*$  is a subsequence of each sequence in a set of sequences  $\mathcal{X} = \{\mathbf{x}_1, \mathbf{x}_2, \dots, \mathbf{x}_n\}$ . (2)  $\mathbf{x}^*$  is the longest among all subsequences that satisfy condition (1). Then we consider  $\mathbf{x}^*$  as the longest common subsequence in  $\mathcal{X}$ .*

If the number of elements in objective set of sequences  $\mathcal{X}$  in this problem is constant, then the solution of the problem is solvable in polynomial time using dynamic programming. Under a situation in which there are only two sequences in  $\mathcal{X}$ , the computational complexity is  $O(nm)$  [14], where  $n, m$  denotes the length of each sequence.

### 2.3 Optimal transport (OT)

Optimal transport provides a means of comparing probability distributions, which are histograms in the finite dimensional case [8, 9]. This quantity is defined over the *same ground space* or multiple pre-registered ground spaces. This comparison is interpreted as a *mass movement problem*, which seeks an optimum plan to move the mass from one distribution to the other at minimal cost. OT is rapidly gaining popularity in a multitude of machine learning problems, ranging from low-rank approximation [15], to dictionary learning [16], domain adaptation [17], clustering [18], and semi-supervised learning [19].

We define two simplexes of histograms with  $n_1$  and  $n_2$  on the same metric space, which are defined, respectively, as  $\Delta_{n_1} = \{\mathbf{p} \in \mathbb{R}_+^{n_1}; \sum_i p_i = 1\}$ , and  $\Delta_{n_2} = \{\mathbf{q} \in \mathbb{R}_+^{n_2}; \sum_j q_j = 1\}$ , where in *mass movement problem*,  $\mathbf{p}, \mathbf{q}$  are usually regarded as mass vectors of each histogram, with elements denoting the mass of each bin. Subsequently, we define two probability measures  $\mu = \sum_{i=1}^{n_1} p_i \delta_{x_i}$ , and  $\nu = \sum_{j=1}^{n_2} q_j \delta_{y_j}$ , where  $x_i \neq x_j$  for  $i \neq j$  is assumed without loss of generality. We also consider the *ground cost matrix*  $\mathbf{C} \in \mathbb{R}_+^{n_1 \times n_2}$ , where  $\mathbf{C}(i, j)$  represents the transportation cost between the  $i$ -th and  $j$ -th element. The optimal transport problem between these two histograms is defined as

$$\mathbf{T}^*(\mathbf{C}, \mathbf{p}, \mathbf{q}) = \arg \min_{\mathbf{T} \in \mathcal{U}_{n_1 n_2}} \langle \mathbf{T}, \mathbf{C} \rangle,$$

where  $\mathcal{U}_{n_1 n_2}$  is defined as

$$\mathcal{U}_{n_1 n_2} := \{\mathbf{T} \in \mathbb{R}_+^{n_1 \times n_2} : \mathbf{T} \mathbf{1}_{n_2} = \mathbf{p}, \mathbf{T}^T \mathbf{1}_{n_1} = \mathbf{q}\},$$

and  $\mathcal{U}_{n_1 n_2}$  represents the polytope of  $n_1 \times n_2$  nonnegative matrices such that their row and column marginals are respectively equal to  $p_i$  and  $q_j$ . This minimization problem involves a linear programming (LP) problem, i.e., a convex optimization problem. Then, the Wasserstein distance between the two measures, denoted as  $\mathcal{W}(\mu, \nu)$ , is equal to the total distance traversed by the mass under the optimal transport plan  $\mathbf{T}^*$ . Furthermore, by adding an entropic regularizer  $H(\mathbf{T}) = -\sum_{i=1}^{n_1} \sum_{j=1}^{n_2} \mathbf{T}(i, j)(\log(\mathbf{T}(i, j)) - 1)$ , a solution of the entropically regularized optimal transport problem is solvable efficiently using Sinkhorn's fixed-point iterations [20, 21, 22]. If no prior information is known about a space, then we set  $\mathbf{p} = \frac{1}{n_1} \mathbf{1}_{n_1}$  and  $\mathbf{q} = \frac{1}{n_2} \mathbf{1}_{n_2}$ .

## 3 Related Work

For graph classification tasks, graph kernel methods have been used widely for several decades. They are also developing rapidly in recent years. Graph kernels are kernel functions that compute similarity between two graphs. Graph kernel methods have shown effective performances in graph classification tasks using machine learning algorithms. In recent years, as effective performances of optimal transport theory in a machine learning domain, graph kernel methods are also improved greatly when combined with optimal transport theory. For now, graph kernel methods can be generally divided into two categories as methods of (1) Traditional graph kernel and (2) OT-based graph kernel.

The first of those classifications of methods includes traditional graph kernels, most of which are based on  $\mathcal{R}$ -convolution framework. To compute similarity between graphs in various data mining tasks, random walk kernel [6] has been developed and used widely as an important tool for graph classification. This method is based on the counting of matching random walks in two graphs with a label or not. However, random walk kernel faces a difficulty by which the computational cost is  $O(n^6)$  for comparing a pair of graphs in graph product space, which is a non-negligible cost,

especially for large-scale graphs. To resolve this difficulty, use of the shortest path kernel [7] has been proposed. It specifically examines a smaller set of shortest paths rather than random walks. Subsequent work on Weisfeiler–Lehman graph kernel [4] has brought great success. They improved the original Weisfeiler–Lehman test using a form of multiple iteration, where neighbor patterns are aggregated. Although this method yields attractive performance, it still presents difficulties of breadth-first strategies and  $\mathcal{R}$ -convolution methods as described in the introduction section.

The second class includes graph kernels combined with optimal transport theory. Recent research by [10], presents a Wasserstein-based Weisfeiler–Lehman graph kernel (WWL), which maps node embedding of a Weisfeiler–Lehman pattern to a feature space, and which computes kernel values using the Wasserstein distance of two point clouds in the feature space. They received better results than those yielded by the original Weisfeiler–Lehman kernel. GOT [23] uses optimal transport differently to compute the Wasserstein distance between two normal distributions derived by graph Laplacian matrices, instead of generating walks or comparing vertex neighbors in graphs. Another attractive work by [24] raises difficulties that both the Wasserstein distance and the Gromov–Wasserstein distance are unable to accommodate the graph structure and feature information. To resolve this difficulty, they propose a notion of Fused Gromov–Wasserstein (FGW) distance, which considers both structure characteristics and feature information of two graphs.

No scheme to apply the OT theory to the path-based graph kernel method has been reported in the relevant literature.

## 4 Longest Common Subsequence (LCS) Kernel

This section proposes a metric between two labeled graphs through comparison of all the shortest path sequences. We will also present a fast kernel in the next section, which has drastically reduced computation. Therefore, we specifically designate this basic method in this section and its fast variant, respectively, as BLCS and FLCS.

### 4.1 Basic concepts

This subsection first introduces several basic concepts in our LCS kernel. They show the operation of transforming the path into a manageable form of data, and a formula of path sequence similarity used in graph comparison procedures.

#### 4.1.1 Shortest path serialization

Given an undirected and connected graph  $G = (\mathcal{V}, \mathcal{E})$  with a set of vertices  $\mathcal{V} = \{v_i\}_{i=1}^N$  and a set of edges  $\mathcal{E} = \{e_{ij}\}$ , then both vertices and edges in  $G$  are assigned a categorical label. To describe the subgraph structure of  $G$ , we choose the shortest path set which contains all shortest paths in  $G$ .

Let  $\mathcal{P}$  denote the shortest path set of  $G$ ,  $\mathcal{P}$  defined as

$$\mathcal{P} \triangleq \{p_{i,j}^* | \forall v_i, v_j \in \mathcal{V}\},$$

where  $p_{i,j}^*$  represents the shortest path from vertex  $v_i$  to  $v_j$ . Assuming that two vertices  $v_k, v_l$  are in the shortest path  $p_{i,j}^*$ , except for the start vertex  $v_i$  and the end vertex  $v_j$ , then  $p_{i,j}^*$  can be expressed as

$$p_{i,j}^* : v_i \xrightarrow{e_{i,k}} v_k \xrightarrow{e_{k,l}} v_l \xrightarrow{e_{l,j}} v_j \quad (1)$$

Because of the difficulty in comparing paths directly, we perform a kind of *shortest path serialization* before path comparison, for which we serialize these paths as *label sequences*. We define the operation of this serialization as



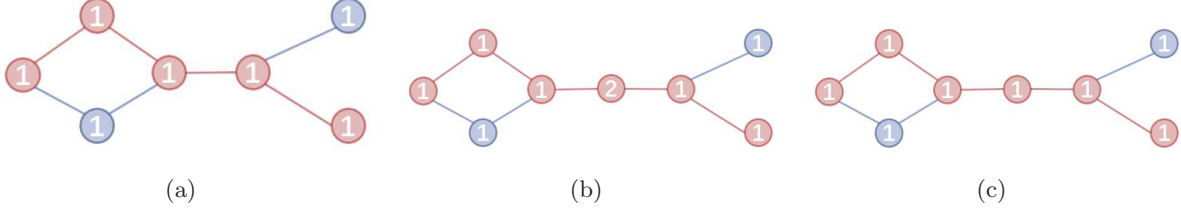


Figure 2: Three similar graphs with vertices labeled, where the vertices and edges in red denote one of the shortest paths in the graph. Notice that the difference between (b) and (c) is that (b) has a vertex with label “2” in the central position.

**Definition 2** (Shortest Path Serialization). *Let  $l : \mathcal{V} \rightarrow \Sigma$  denote a function that maps a vertex object  $v$  to its categorical node label assigned from a finite label alphabet  $\Sigma$ . Furthermore, let  $w : \mathcal{E} \rightarrow \Sigma$  be the edge label mapping function. The operation of shortest path serialization is definable as (take  $p_{i,j}^*$  in Eq. (1) for instance):*

$$\mathbf{x} = (l(v_i), -w(e_{i,k}), l(v_k), -w(e_{k,l}), l(v_l), -w(e_{l,j}), l(v_j)),$$

where  $\mathbf{x}$  is a shortest path sequence derived from  $p_{i,j}^*$ . In the special condition in which the graph has no edge label,  $p_{i,j}^*$  is serialized as  $\mathbf{x} = (l(v_i), l(v_k), l(v_l), l(v_j))$ .

It is noteworthy that we take the negative value of edge label as  $-w(e_{i,j})$  so that edge labels are distinguished from node labels during path sequence comparison.

#### 4.1.2 Path sequence similarity

Using shortest path serialization, we transform the path comparison problem to a sequence comparison problem. As described earlier, to make use of a path sequence maximally, we solve the substructure isomorphism problem of paths instead of simply judging whether or not these two paths are completely identical.

As sequence comparison strategies, many methods might be chosen, such as longest common substring (LCStr) and longest common subsequence (LCSeq). The difference between them is that the LCStr demands continuity of sequence above LCSeq. We prefer to use LCSeq rather than LCStr because we discover LCSeq as typically more robust and stable than LCStr. Assume three graphs with vertices labeled like graph (a), (b) and (c) in Figure 2, where the vertices and edges in red denote one of the shortest paths in the graph. Generally, these three graphs should be considered as similar to each other. However, the output of LCSeq and LCStr differs a lot. Through shortest path serialization, these three shortest paths in graph (a), (b) and (c) are serialized as three path sequences  $\mathbf{x}_a = (1, 1, 1, 1, 1)$ ,  $\mathbf{x}_b = (1, 1, 1, 2, 1, 1)$  and  $\mathbf{x}_c = (1, 1, 1, 1, 1, 1)$  respectively. The longest common substructure using LCSeq and LCStr are showed in Table 1. As we can see, in the case of comparing  $\mathbf{x}_a, \mathbf{x}_b$  and  $\mathbf{x}_b, \mathbf{x}_c$ , the length of LCStr suddenly reduce since a point with label of 2 suddenly shows up in the  $\mathbf{x}_b$ . Thus LCStr are more likely to be cut off by unmatched vertices.

Using the length of LCSeq, we propose our formula of path sequence similarity as

**Definition 3** (Path Sequence Similarity). *Given two path sequences  $\mathbf{x}_1, \mathbf{x}_2$ , their similarity is defined as*

$$F_{\text{sim}}(\mathbf{x}_1, \mathbf{x}_2) := \frac{F_{\text{lcs}}(\mathbf{x}_1, \mathbf{x}_2)}{\max(\text{len}(\mathbf{x}_1), \text{len}(\mathbf{x}_2))}, \quad (2)$$

where  $F_{\text{lcs}}(\mathbf{x}_1, \mathbf{x}_2)$  represents the function that returns the length of the Longest Common Subsequence of  $\mathbf{x}_1, \mathbf{x}_2$ , and where  $\text{len}(\cdot)$  denotes the function returning the length of a sequence.

Table 1: Longest common substructure using different comparing strategies. Each item in these tables denote a comparing result of two path sequences derived from examples in Figure 2. Table (a) shows them in the form of sequence, table (b) shows the length of longest common substructures.

(a)			
Methods	$\mathbf{x}_a, \mathbf{x}_b$	$\mathbf{x}_a, \mathbf{x}_c$	$\mathbf{x}_b, \mathbf{x}_c$
LCSeq	(1,1,1,1,1)	(1,1,1,1,1)	(1,1,1,1,1)
LCStr	(1,1,1)	(1,1,1,1,1)	(1,1,1)

(b)			
Methods	$\mathbf{x}_a, \mathbf{x}_b$	$\mathbf{x}_a, \mathbf{x}_c$	$\mathbf{x}_b, \mathbf{x}_c$
LCSeq	5	5	5
LCStr	3	5	3

We use the maximum length of the objective path sequences as a denominator to limit its value in  $[0, 1]$ . When two path sequences have a longer common subsequence, the value of their similarity will be larger. From the perspective of the graph, large similarity of path sequences shows large similarity of subgraph structures.

## 4.2 BLCS Kernel in graph comparing

### 4.2.1 Generating graph representation

Given two undirected and connected graphs  $G_1(\mathcal{V}_1, \mathcal{E}_1)$  and  $G_2(\mathcal{V}_2, \mathcal{E}_2)$  with nodes and edges labeled, then using a classical algorithm like Floyd–Warshall or the Dijkstra algorithm, the shortest path sets  $\mathcal{P}_1$  and  $\mathcal{P}_2$  of  $G_1$  and  $G_2$  can be obtained, respectively. Through shortest path serialization, we first transform all paths in  $\mathcal{P}_1$  and  $\mathcal{P}_2$  as shown below. It should be noted that in the situation where there is not only one shortest path exists for two certain vertices, we only use one of them randomly, which is determined by the shortest path algorithm like Floyd–Warshall or Dijkstra algorithm.

$$\begin{aligned}\mathcal{X}_1 &= \left\{ \mathbf{x}_{i,j}^{(1)} \mid \mathbf{x}_{i,j}^{(1)} = F_{\text{serialize}}(p_{i,j}^*, p_{i,j}^* \in \mathcal{P}_1) \right\} \\ \mathcal{X}_2 &= \left\{ \mathbf{x}_{i,j}^{(2)} \mid \mathbf{x}_{i,j}^{(2)} = F_{\text{serialize}}(p_{i,j}^*, p_{i,j}^* \in \mathcal{P}_2) \right\}\end{aligned}$$

Therein,  $F_{\text{serialize}}$  denotes the operation of shortest path serialization described earlier. Actually,  $\mathcal{X}_1$  and  $\mathcal{X}_2$  respectively represent two path sequence sets derived from  $\mathcal{P}_1$  and  $\mathcal{P}_2$ , respectively describing the subgraph structures of  $G_1$  and  $G_2$ . For every path sequence  $\mathbf{x}_{i,j}^{(1)}$  and  $\mathbf{x}_{i,j}^{(2)}$ , the superscript denotes the graph to which they belong.

It is noteworthy that some path sequences that are exactly the same as those in the path sequence set. To avoid the increase of the identical sequences, we do not add them to the sequence set  $\mathcal{X}$  and store the number of identical sequences in a mass vector  $\mathbf{m}$ . For example, the  $i$ -th element in  $\mathbf{m}$  denotes the number of sequences which are identical to the  $i$ -th path sequence in  $\mathcal{X}$ . In doing so, we obtain two mass vectors  $\mathbf{m}_1$  and  $\mathbf{m}_2$  respectively belonging to  $\mathcal{X}_1$  and  $\mathcal{X}_2$ .

### 4.2.2 Wasserstein Distance in LCS metric space

To compare path sequence sets  $\mathcal{X}_1$  and  $\mathcal{X}_2$ , we propose a metric space of path sequence over the union of  $\mathcal{X}_1$  and  $\mathcal{X}_2$ , where we use path sequence similarity to define the metric.



**Definition 4** (LCS Metric Space). *Given two path sequence sets  $\mathcal{X}_1, \mathcal{X}_2$ , and  $\mathcal{X} := \mathcal{X}_1 \cup \mathcal{X}_2$  is their union. The LCS Metric Space of  $\mathcal{X}_1$  and  $\mathcal{X}_2$  is written as  $S(\mathcal{X}, d)$ , where the metric  $d : \mathcal{X} \times \mathcal{X} \rightarrow \mathbb{R}$  is defined as shown below.*

$$d(\mathbf{x}_1, \mathbf{x}_2) = 1 - F_{\text{sim}}(\mathbf{x}_1, \mathbf{x}_2) \quad (3)$$

**Theorem 1.** *The metric function  $d : \mathcal{X} \times \mathcal{X} \rightarrow \mathbb{R}$  of LCS metric space is a metric.*

Actually,  $\mathcal{X}_1$  and  $\mathcal{X}_2$  can be regarded as two distributions in their LCS Metric Space, where the path sequence is a discrete point of these distributions. Finally, we propose to leverage the Wasserstein distance between these two distributions to define our graph distance as

**Definition 5** (LCS Graph Distance). *Given two undirected and connected graphs  $G_1(\mathcal{V}_1, \mathcal{E}_1)$  and  $G_2(\mathcal{V}_2, \mathcal{E}_2)$  and their respective path sequence sets  $\mathcal{X}_1$  and  $\mathcal{X}_2$  and mass vectors  $\mathbf{m}_1$  and  $\mathbf{m}_2$ , then the LCS Graph Distance between  $G_1$  and  $G_2$  is defined as*

$$d_G(G_1, G_2) = \mathcal{W}_1(\mathcal{X}_1, \mathcal{X}_2) = \langle \mathbf{T}^*(\mathbf{D}, \frac{\mathbf{m}_1}{\|\mathbf{m}_1\|_1}, \frac{\mathbf{m}_2}{\|\mathbf{m}_2\|_1}), \mathbf{D} \rangle$$

where  $\mathcal{W}_1(\mathcal{X}_1, \mathcal{X}_2)$  represents the 1-Wasserstein distance between distribution  $\mathcal{X}_1$  and  $\mathcal{X}_2$ , and where  $\mathbf{D}$  denotes the ground distance matrix including the distances  $d(\mathbf{x}_1, \mathbf{x}_2)$  between  $\mathbf{x}_1 \in \mathcal{X}_1$  and  $\mathbf{x}_2 \in \mathcal{X}_2$  in the LCS Metric Space  $S(\mathcal{X}_1 \cup \mathcal{X}_2, d)$ . Here,  $\mathbf{T}^*(\mathbf{D}, \frac{\mathbf{m}_1}{\|\mathbf{m}_1\|_1}, \frac{\mathbf{m}_2}{\|\mathbf{m}_2\|_1})$  denotes the optimal transport plan w.r.t. mass vectors  $\mathbf{m}_1$  and  $\mathbf{m}_2$  of  $\mathcal{X}_1$  and  $\mathcal{X}_2$ , respectively, and  $\mathbf{D}$ , where  $\|\cdot\|_1$  denotes the  $l_1$  norm.

We use LCS graph distance to compute a similarity measure between two graphs. The measure will be used in machine learning algorithm as a kernel value. Here we combine the LCS graph distance with the Laplacian kernel function to construct a graph kernel. The LCS graph kernel is then defined as presented below. The proofs of Theorem 1 is provided in the next subsection.

**Definition 6.** *Given a set of graphs  $\mathcal{G}$ , then  $G_i$  and  $G_j$  are two arbitrary graphs in  $\mathcal{G}$ . The LCS graph kernel is defined as*

$$k_{\text{LCS}}(G_i, G_j) = e^{-\lambda d_G(G_i, G_j)}, \quad (4)$$

where  $d_G$  denotes the LCS graph distance, and where  $\lambda$  is within the range of  $(0, +\infty]$ .

### 4.3 Proof of Theorem 1

In this subsection, we will prove some important propositions about LCS metric space.

We give a self-contained proof of **Theorem 1** by exactly following the results of previous work [25], which also proposes an LCS-based string metric similar to ours. We first restate the definition of metric before proceeding.

**Definition 7** (Metric). *A metric on the set  $\mathcal{X}$  is a function  $d : \mathcal{X} \times \mathcal{X} \rightarrow \mathbb{R}$  that satisfies the following properties for all  $x, y, z \in \mathcal{X}$ :*

- (1) *Positive definiteness:*  $d(x, y) \geq 0$ , and  $d(x, y) = 0$  if and only if  $x = y$ ;
- (2) *Symmetry:*  $d(x, y) = d(y, x)$ ;
- (3) *Triangle inequality:*  $d(x, y) \leq d(x, z) + d(z, y)$

To prove the LCS metric of LCS metric space  $d(\mathbf{x}_1, \mathbf{x}_2) = 1 - \frac{F_{\text{LCS}}(\mathbf{x}_1, \mathbf{x}_2)}{\max(\text{len}(\mathbf{x}_1), \text{len}(\mathbf{x}_2))}$  (Equation (2) and (3) in the paper) is a metric, we only have to prove the following lemmas:

**Lemma 1.** *The function of LCS metric is positive definite and symmetric.*

*Proof.* Because longest common subsequence is a subsequence of its parent sequences, it means that  $\frac{F_{\text{LCS}}(\mathbf{x}_1, \mathbf{x}_2)}{\max(\text{len}(\mathbf{x}_1), \text{len}(\mathbf{x}_2))} \leq 1$  and  $F_{\text{LCS}}(\mathbf{x}_1, \mathbf{x}_2) = \max(\text{len}(\mathbf{x}_1), \text{len}(\mathbf{x}_2))$  if and only if  $\mathbf{x}_1 = \mathbf{x}_2$ . Therefore,  $d(\mathbf{x}_1, \mathbf{x}_2) \geq 1 - 1 = 0$ , and  $d(\mathbf{x}_1, \mathbf{x}_2) = 0$  if and only if  $\mathbf{x}_1 = \mathbf{x}_2$ . Thus the function of LCS metric is positive definite.

As for the symmetry, because longest common subsequence method does not care about the order of compared parent sequences, we have  $d(\mathbf{x}_1, \mathbf{x}_2) = d(\mathbf{x}_2, \mathbf{x}_1)$ . Subsequently, the function of LCS metric is symmetric. This completes the proof.  $\square$

**Lemma 2.** *The function of LCS metric satisfies the triangle inequality.*

Before proceeding, we first restate an important proposition of longest common subsequence proving by Bakkelund [25].

**Proposition 1** (Lemma 3.3 and Corollary 3.4 in [25]). *The following inequality holds for all  $\mathbf{x}, \mathbf{y}, \mathbf{z} \in \mathcal{X}$ , where  $\mathcal{X}$  is a certain sequence set:*

$$F_{\text{LCS}}(\mathbf{x}, \mathbf{y}) + F_{\text{LCS}}(\mathbf{y}, \mathbf{z}) - F_{\text{LCS}}(\mathbf{x}, \mathbf{z}) \leq \text{len}(\mathbf{y}).$$

*Proof.* Because the symmetry of LCS metric  $d(\mathbf{x}, \mathbf{y})$  is proved in **Lemmas 1**, we can safely assume that  $\text{len}(\mathbf{x}) \leq \text{len}(\mathbf{z})$  in the triangle inequality as follows:

$$d(\mathbf{x}, \mathbf{z}) \leq d(\mathbf{x}, \mathbf{y}) + f(\mathbf{y}, \mathbf{z}), \quad (5)$$

where  $\mathbf{x}, \mathbf{y}, \mathbf{z} \in \mathcal{X}$ . Thus we have  $M(\mathbf{x}, \mathbf{y}) \leq M(\mathbf{y}, \mathbf{z})$  and  $M(\mathbf{x}, \mathbf{z}) \leq M(\mathbf{y}, \mathbf{z})$ , where  $M(\mathbf{x}, \mathbf{y}) = \max(\text{len}(\mathbf{x}), \text{len}(\mathbf{y}))$ . Due to **Proposition 1**, we can derive:

$$\begin{aligned} M(\mathbf{x}, \mathbf{y})(F_{\text{LCS}}(\mathbf{y}, \mathbf{z}) - F_{\text{LCS}}(\mathbf{x}, \mathbf{z})) &\leq M(\mathbf{y}, \mathbf{z})(\text{len}(\mathbf{y}) - F_{\text{LCS}}(\mathbf{x}, \mathbf{y})) \\ \iff F_{\text{LCS}}(\mathbf{x}, \mathbf{y})M(\mathbf{y}, \mathbf{z}) + F_{\text{LCS}}(\mathbf{y}, \mathbf{z})M(\mathbf{x}, \mathbf{y}) &\leq \text{len}(\mathbf{y})M(\mathbf{y}, \mathbf{z}) + F_{\text{LCS}}(\mathbf{x}, \mathbf{z})M(\mathbf{x}, \mathbf{y}). \end{aligned}$$

Because we have  $M(\mathbf{x}, \mathbf{z}) \leq M(\mathbf{y}, \mathbf{z})$ , we can derive that:

$$\begin{aligned} &F_{\text{LCS}}(\mathbf{x}, \mathbf{y})M(\mathbf{y}, \mathbf{z}) + F_{\text{LCS}}(\mathbf{y}, \mathbf{z})M(\mathbf{x}, \mathbf{y}) \\ &\leq M(\mathbf{x}, \mathbf{y})M(\mathbf{y}, \mathbf{z}) + F_{\text{LCS}}(\mathbf{x}, \mathbf{z})M(\mathbf{x}, \mathbf{y}) \frac{M(\mathbf{y}, \mathbf{z})}{M(\mathbf{x}, \mathbf{z})}. \end{aligned}$$

Then we can obtain the following by dividing both sides of inequality above by  $M(\mathbf{x}, \mathbf{y})M(\mathbf{y}, \mathbf{z})$ :

$$\begin{aligned} \frac{F_{\text{LCS}}(\mathbf{x}, \mathbf{y})}{M(\mathbf{x}, \mathbf{y})} + \frac{F_{\text{LCS}}(\mathbf{y}, \mathbf{z})}{M(\mathbf{y}, \mathbf{z})} &\leq 1 + \frac{F_{\text{LCS}}(\mathbf{x}, \mathbf{z})}{M(\mathbf{x}, \mathbf{z})} \\ \iff 1 - \frac{F_{\text{LCS}}(\mathbf{x}, \mathbf{z})}{M(\mathbf{x}, \mathbf{z})} &\leq 1 - \frac{F_{\text{LCS}}(\mathbf{x}, \mathbf{y})}{M(\mathbf{x}, \mathbf{y})} + 1 - \frac{F_{\text{LCS}}(\mathbf{y}, \mathbf{z})}{M(\mathbf{y}, \mathbf{z})}. \end{aligned}$$

Thus Eq. (5) holds for all  $\mathbf{x}, \mathbf{y}, \mathbf{z} \in \mathcal{X}$ , and the length between any two of them is not equal to zero. Actually, we do not consider the situation that a sequence is empty, because there exists no shortest path of which length is equal to zero.  $\square$

Consequently, the proof of **Theorem 1** is finally given as presented below:

*Proof.* From **Lemmas 1**, the function of LCS metric is positive definite and symmetric. Also, **Lemmas 2** guarantees that the function of LCS metric satisfies the triangle inequality. Therefore, LCS metric satisfies the axiom for a metric. This completes the proof.  $\square$

## 4.4 Time complexity

We discuss the time complexity of the BLCS kernel by dividing the algorithm into two parts. In the first part, the algorithm first generates a path sequence set for graph representation. In the BLCS kernel, we use all shortest paths in an undirected and connected graph. Assuming that the objective graph has  $N$  vertices, then the time complexity for graph representation generation is  $O(N^2)$  for each graph. Furthermore,  $N^2$  path sequences are obtained after graph representation generation. In the second part, the algorithm performs one-to-one comparison of path sequences of two graphs to compute the ground distance matrix for calculating the Wasserstein distance. Using dynamic programming, one time of LCS computing is cost computation in  $O(l^2)$ , where  $l$  denotes the average length  $l$  of path sequences. Under this situation, performing one-to-one comparison will require computation in  $O(N^4l^2)$ .

## 5 Fast LCS Kernel

We present a fast LCS (FLCS) graph kernel based on adjacent point merging in the LCS metric space. It is noteworthy that this greatly reduces computational costs while preserving (sometimes improving) the BLCS kernel accuracy.

### 5.1 Improving strategies

Through comparison of shortest path sequences in a single graph, we discovered that many similar but not completely identical shortest path sequence samples are repeated. This repetition might cause unnecessarily redundant calculations for comparison. Moreover, the finally obtained ground distance matrix might exacerbate degradation of classification performances. To alleviate these issues in the BLCS kernel, we propose two strategies: fragmented path sequences removing and adjacent point merging, and specifically addressing reduction of the path sequence set size.

#### 5.1.1 Fragmented path sequence removal

The fragmented path sequences are those sequences having negligible length, which are short because they carry only limited information. Dealing with these path sequences might not only cause unnecessary computation; it might also bring negative effects on Wasserstein distance calculation. Therefore, we perform a fragmented path sequence removal as preprocessing.

Given a path sequence set  $\mathcal{X}$  with  $N^2$  shortest path sequences included, we reconstruct  $\mathcal{X}$  with length-limited conditions as

$$\mathcal{X}_{\text{new}} = \{\mathbf{x}_i | \mathbf{x}_i \in \mathcal{X}, \text{len}(\mathbf{x}_i) \geq \rho \cdot L_{\max}\},$$

where  $L_{\max}$  denotes the length of the longest one among all path sequences in  $\mathcal{X}$ , and where  $\rho$  is the parameter of the removing ratio, valued within as  $(0, 1)$ . When  $\rho = 0$ , meaning that all of the path sequences in original  $\mathcal{X}$  will be reserved. When  $\rho = 1$ , only the path sequences having longest length will be reserved.

#### 5.1.2 Adjacent point merging in LCS metric space

As described above, path sequences in the original  $\mathcal{X}$  are redundant to a certain degree. We can observe this point in the LCS metric space as Figure 3(a), where points in a distribution are usually numerous and dense. Actually, when we map an original shortest path sequence set of a graph to

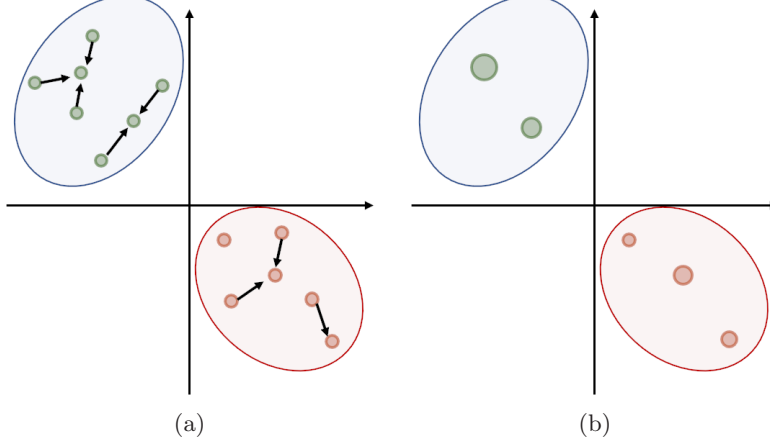


Figure 3: Visual summary of adjacent point merging, where blue and red areas denote two distributions in LCS metric space and where the point size shows their mass: (a) two distributions before point merging, arrows show the merging direction; and (b) the same distributions after merging, where the adjacent points are combined, as are their masses.

the LCS metric space, these points in the distribution are usually close to a local center and are divisible into several parts.

Consequently, aiming at reducing the density of points in metric space, we propose an operation of adjacent point merging because the Wasserstein distance considers mass of discrete point in distribution. For this purpose, we follow the same strategy of recalculation of the mass vector as that used for BLCS. As shown in Figure 3, points in distributions are merged to their local center. Masses of merged points will also be accumulated to the local center. They appear to grow larger in Figure 3(b).

**Definition 8** (Adjacent Point Merging). *Given a discrete distribution  $\mathcal{X}$  in LCS metric space  $S(\mathcal{X}, d)$ , with parameter  $s$  as merging radius, then each point in  $\mathcal{X}$  is assigned an equivalent mass 1. Subsequently, we define a set  $\mathcal{X}'$  to store local center points and to add a random point in it. For the remainder of points in  $\mathcal{X}$ , we define the merging attempt as shown below.*

$$F_{\text{attempt}}(\mathbf{x}) = \begin{cases} 1, & \min_{\mathbf{x}' \in \mathcal{X}'} d(\mathbf{x}, \mathbf{x}') \leq s \\ 0, & \min_{\mathbf{x}' \in \mathcal{X}'} d(\mathbf{x}, \mathbf{x}') > s. \end{cases}$$

*We perform merging attempts on points in the original distribution. If we obtain  $F_{\text{attempt}}(\mathbf{x}) = 1$ , then  $\mathbf{x}$  will be merged with the local center  $\mathbf{x}' = \arg \min_{\mathbf{x}' \in \mathcal{X}'} d(\mathbf{x}, \mathbf{x}')$ , with their mass combined as  $m' := m' + m$ , where  $m', m$  denotes the mass of  $\mathbf{x}', \mathbf{x}$ . If we get  $F_{\text{attempt}}(\mathbf{x}) = 0$ , then  $\mathbf{x}$  will be regarded as a new local center and added to  $\mathcal{X}'$ . Eventually, a merged distribution  $\mathcal{X}'$  with mass vector  $\mathbf{m}$  of all remaining points is obtained.*

As a result of adjacent point merging, Figure 3(b) shows that the original dense distributions are converted to new distributions including fewer points with combined mass. After obtaining  $\mathcal{X}$  and  $\mathbf{m}$ , the FLCS kernel follows the same step of BLCS to compute kernel values.

## 5.2 Time complexity

Similarly to the BLCS kernel, we discuss time complexity of the FLCS kernel under the same assumption. In the first part, for adjacent point merging, we consider the worst situation with

$\frac{N(N+1)}{2}$  times comparison. An adjacent point combination will cost a maximum computational cost in  $O(N^2l^2)$ . In the second part, assuming that  $K$  path sequences remain after adjacent point merging, the path sequence comparing of two graphs will cost  $O(K^2l^2)$ . The time complexity for the FLCs kernel is  $O(N^2l^2 + K^2l^2)$ . This time complexity is reduced dramatically by comparison to  $O(N^4)$  in the BLCS kernel. We also conduct numerical evaluations to compare elapsed times with other state-of-the-art methods as presented in the next section.

## 6 Algorithm

In this section, we will present the algorithm details of some key operations in the BLCS kernel and the FLCs kernel.

Algorithm 1 shows the implement details of path sequence set computing. The concatenate( $\mathbf{x}, \mathbf{y}$ ) function here concatenating two sequences  $\mathbf{x}, \mathbf{y}$  together using a push-back operation.

Algorithm 2 shows the implement details of graph representation computing in BLCS kernel, which outputs the path sequence set  $\mathcal{X}$  and its mass vector  $\mathbf{m}$ .  $\mathbf{m}(k)$  denotes the k-th element of  $\mathbf{m}$ .

---

### Algorithm 1 Compute shortest path serialization

---

**Input:** Shortest path  $p_{i,j}^*$  in graph  $\mathcal{G} = \{\mathcal{V}, \mathcal{E}\}$ ; vertices  $v_i \in \mathcal{V}$ ; edges of  $v_i$  and  $v_j$ :  $e_{i,j} \in \mathcal{E}$ ; mapping function of categorical node label  $l(v)$ ; mapping function of categorical edge label  $w(e)$ .

**Output:** Shortest path sequence  $\mathbf{x}_{i,j}$ .

- 1:  $\mathbf{x}_{i,j} \leftarrow \text{null}$  // Initialize the path sequence of  $p_{i,j}^*$
  - 2: **for**  $v_k$  **in**  $p_{i,j}^*$  **do** // Operate each node
  - 3:    $\mathbf{x}_{i,j} \leftarrow \text{concatenate}(\mathbf{x}_{i,j}, l(v_k))$   
      // Concatenate  $\mathbf{x}_{i,j}$  with next node label
  - 4:   **if**  $v_k$  is not the last node **then**
  - 5:      $\mathbf{x}_{i,j} \leftarrow \text{concatenate}(\mathbf{x}_{i,j}, -w(e_{k,k+1}))$   
      // Concatenate  $\mathbf{x}_{i,j}$  with next edge label
  - 6:   **end if**
  - 7: **end for**
-

---

**Algorithm 2** Compute graph representation in basic method

---

**Input:** Objective graphs  $G = (\mathcal{V}, \mathcal{E})$ .

**Output:** Path sequence set  $\mathcal{X}$ ; mass vector  $\mathbf{m}$ .

```
1:  $\mathcal{X}, \mathbf{m} \leftarrow null$ 
   // Initialize the shortest path sequence set of  $\mathcal{G}$ 
2:  $\mathcal{P} \leftarrow$  Compute shortest path set
3: for  $p_{i,j}^*$  in  $\mathcal{P}$  do
4:    $\mathbf{x}_{i,j} \leftarrow F_{\text{serialize}}(p_{i,j}^*)$ 
   // Serialize each shortest path
5:   if  $\exists \mathbf{x}_k \in \mathcal{X}, \mathbf{x}_k == \mathbf{x}_{i,j}$  then
6:      $\mathbf{m}(k) \leftarrow \mathbf{m}(k) + 1$ 
7:   else
8:      $\mathbf{m} \leftarrow \text{concatenate}(\mathbf{m}, 1)$ 
9:      $\mathcal{X} \leftarrow \mathcal{X} \cup \mathbf{x}_{i,j}$ 
   // Add path sequence  $\mathbf{x}_{i,j}$  to the set
10:  end if
11: end for
```

---

---

**Algorithm 3** Compute graph representation in fast method

---

**Input:** Objective graphs  $G = (\mathcal{V}, \mathcal{E})$ ; removing ratio  $\rho \in [0, 1]$ ; combination radius  $s \in [0, 1]$ .

**Output:** Path sequence set  $\mathcal{X}$ ; mass vector  $\mathbf{m}$ .

```
1:  $\mathcal{X}, \mathbf{m} \leftarrow null$ 
2:  $\mathcal{P}, L_{\max} \leftarrow$  Compute shortest path set of  $G$  and the length of the longest one
3: for  $p_{i,j}^*$  in  $\mathcal{P}$  do
4:   if  $\text{len}(p_{i,j}^*) \leq \rho L_{\max}$  then
5:     continue // Removing fragmented paths
6:   end if
7:    $\mathbf{x}_{i,j} \leftarrow F_{\text{serialize}}(p_{i,j}^*)$ 
   // Serialize each shortest path
8:    $\mathbf{x}_k, m_k \leftarrow$  the nearest point of  $\mathbf{x}_{i,j}$  in  $\mathcal{X}$  and its mass
9:   if  $\mathcal{X} \neq null$  and  $d(\mathbf{x}_k, \mathbf{x}_{i,j}) \leq s$  then
10:     $\mathbf{x}_k \leftarrow$  the lonest one among  $\mathbf{x}_k, \mathbf{x}_{i,j}$ 
11:     $\mathbf{m}(k) \leftarrow \mathbf{m}(k) + 1$ 
   // Combine the masses of  $\mathbf{x}_k, \mathbf{x}_{i,j}$ 
12:  else
13:     $\mathbf{m} \leftarrow \text{concatenate}(\mathbf{m}, 1)$ 
14:     $\mathcal{X} \leftarrow \mathcal{X} \cup \mathbf{x}_{i,j}$  // Add  $\mathbf{x}_{i,j}$  as a new point to  $\mathcal{X}$ 
15:  end if
16: end for
```

---

Algorithm 3 shows the implement details of the improved way to compute the path sequence set  $\mathcal{X}$  and mass vector  $\mathbf{m}$  by performing fragmented path removing and adjacent point merging.

Algorithm 4 shows the implementation of computing LCS kernel value. We here use sinkhorn method to solve optimal transport problem with ground distance matrix  $\mathbf{D}$ . We also use the Laplacian Kernel Function with parameter  $\lambda$  to calculate kernel value.



---

**Algorithm 4** Compute LCS kernel value

---

**Input:** Two objective path sequence sets  $\mathcal{X}_1, \mathcal{X}_2$ ; mass vectors  $\mathbf{m}_1, \mathbf{m}_2; \lambda$ .

**Output:** LCS kernel value  $k_{\text{LCS}}(G_1, G_2)$

```
1:  $\mathbf{D} \leftarrow null$  // Initialize cost matrix of transporting  $\mathcal{X}_1, \mathcal{X}_2$ 
2: for  $\mathbf{x}_i^{(1)}$  in  $\mathcal{X}_1$  do
3:   for  $\mathbf{x}_j^{(2)}$  in  $\mathcal{X}_2$  do
4:      $\mathbf{D}(i, j) \leftarrow 1 - \frac{F_{\text{LCS}}(\mathbf{x}_i^{(1)}, \mathbf{x}_j^{(2)})}{\max(\text{len}(\mathbf{x}_i^{(1)}), \text{len}(\mathbf{x}_j^{(2)}))}$ 
        // Compute ground distance matrix of  $\mathbf{x}_i^{(1)}, \mathbf{x}_j^{(2)}$  in LCS metric space
5:   end for
6: end for
7:  $\mathbf{T}^* \leftarrow \text{sinkhorn}(\mathbf{D}, \frac{\mathbf{m}_1}{|\mathbf{m}_1|}, \frac{\mathbf{m}_2}{|\mathbf{m}_2|})$ 
        // Use sinkhorn method to compute optimal transport plan  $\mathbf{T}^*$ 
8:  $d_G \leftarrow \langle \mathbf{T}^*, \mathbf{D} \rangle$  // Compute the Wasserstein distance
9:  $k_{\text{LCS}}(G_1, G_2) \leftarrow e^{-\lambda d_G}$ 
```

---

## 7 Numerical Evaluation

This section compares our method with other state-of-the-art graph classification methods by performance of numerical experiments. Particularly, this evaluation reveals that the proposed BLCS and FLCS kernels outperform many state-of-the-art methods in most widely used datasets.

### 7.1 Datasets

For real-world datasets, we use several widely used benchmark datasets. Among them, MUTAG [26], PTC-FM, PTC-MR [27] and AIDS [28] include graphs with discrete labels of both vertices and edges. MSRC-9, MSRC-21, MSRC-21C [29] include graphs with discrete vertex labels. BZR, COX2 [30], ENZYMES [31], and PROTEINS [32] include graphs with discrete and continuous vertex attributes. Also, BZR-MD, COX2-MD, and ER-MD [30] include graphs with discrete labels of vertices and with both discrete and continuous attributes of edges. The IMDB-B and IMDB-M [33] datasets include both unlabeled and unattributed graphs. All datasets above are available in [34].

Table 2: Statistical information of datasets

Dataset	Cat.	Graphs	Classes	Avg. $ \mathcal{V} $	Avg. $ \mathcal{E} $
MUTAG	bio	188	2	17.93	19.79
PTC-FM	bio	349	2	14.11	14.48
PTC-MR	bio	344	2	14.29	14.69
AIDS	bio	2000	2	15.69	16.20
BZR	bio	405	2	35.75	38.36
COX2	bio	467	2	41.22	43.45
ENZYMES	bio	600	6	32.63	62.14
PROTEINS	bio	1113	2	39.06	72.82
BZR-MD	bio	405	2	21.30	225.06
COX2-MD	bio	303	2	26.28	335.12
ER-MD	bio	446	2	21.33	234.85
MSRC-9	cv	221	8	40.58	97.94
MSRC-21	cv	563	20	77.52	198.32
MSRC-21C	cv	209	20	40.28	96.60
IMDB-B	soc	1000	2	19.77	96.53
IMDB-M	soc	1500	3	13.00	65.94

Table 2 shows the specific information of datasets which we use. We divide datasets into two categories according to their sources as *bio*, *cv* and *soc*, which denote bioinformatics, computer vision and social network, respectively. The Avg. $|\mathcal{V}|$  and Avg. $|\mathcal{E}|$  columns show the average number of vertices and edges in a dataset, respectively, where we can see that the datasets BZR-MD, COX2-MD and ER-MD are dense graph datasets.

Because our proposed method only supports graphs with discrete labels of vertices and/or edges, we apply some preprocessing before experiments: (1) we remove continuous attributes from original graphs, making sure that only discrete labels remain; (2) for those unlabeled graphs, we use the degree measures of the respective vertices as attributes.

## 7.2 Experiment setup

For numerical experiments, we test both BLCS and FLCS kernel to evaluate our improving strategies. For the FLCS kernel, we set up a grid search to find the best pair of parameters, where the removing ratio  $\rho$  is within  $\{0.6, 0.8, 1\}$  and the merging radius  $s$  is within  $\{0, 0.2, 0.5, 0.8\}$ .

We compare results obtained using our methods with those from other methods of three categories: (1) traditional graph kernel, (2) OT-based graph kernel, and (3) graph embedding method. In the first category, we choose the Weisfeiler–Lehman Kernel (WLK), Random Walk Kernel (RWK), and Shortest Path Kernel (SPK), which we described in the related work section. For implementation of all the traditional graph kernels, we use the Grakel python library [35]. For the second category, we choose the Wasserstein–Weisfeiler–Lehman Kernel (WWL) and Fused Gromov–Wasserstein Kernel (FGW). For the last category, we choose the Anonymous Walk Embeddings (AWE) [36], which is a graph-embedding method based on anonymous walks in a graph. The parameter of  $H$  in WLK and WWL is set as 4. The shortest path matrix is used in FGW. For all kernel methods based on Laplacian kernel, we use the best parameter  $\lambda$  within  $\{0.0001, 0.001, 0.01, 0.1, 1, 10\}$ .

For classification, we train a multi-class SVM classifier using one-vs.-one approach, and apply 10

times of 10-fold cross-validation, which is 100 times classification in all. For parameter adjustment of SVM, we apply a grid search with SVM parameter  $C$  within  $\{0.001, 0.01, 0.1, 1, 10, 100, 1000\}$  for every cross-validation. Then we calculate an average accuracy and a standard deviation after classification. We run these experiments on a machine with Intel Core i7 CPU with 2.60 GHz and 16 GB RAM.

### 7.3 Classification on different datasets

We perform classification experiments on datasets belonging to different categories. Tables 3, 4, 5 and 6 show the average classification accuracies on graphs, where the top two accuracies of each dataset are in bold. It should be noted that the results marked with “-” indicate that dataset is not applicable for objective method.

Overall, our proposed methods are shown to outperform many state-of-the-art methods in some datasets. They also keep good performance on most datasets. As shown in Tables 3, 4 and 5, in normal datasets such as MUTAG, COX2, MSRC-9, MSRC-21, MSRC-21C, ENZYMES and IMDB-B, our proposed methods perform the best. We also find that in some datasets of computer vision category (MSRC-9, MSRC-21, MSRC-21C), our proposed methods outperform a lot than other well-known Weisfeiler–Lehman–based methods like WL and WWL.

We also perform dense graph experiments that test our proposed methods on a dataset with dense graphs, as shown in Table 6, where our proposed method also retains good performances. Furthermore, elapsed time experiments are presented in Table 7, where we use  $\rho = 0.8, s = 0.5$  for FLCS kernel. From Table 7, we find that the FLCS kernel has greatly reduced computational cost from BLCS kernel, also that it is competitive in computational speed among ot-based methods.

### 7.4 Classification under different parameters

To evaluate the classification performance of FLCS, the fast variant of the proposed method under different pairwises of parameter, we set up several parameter adjustment experiments. In the experiments, we change one of the parameters and leave the other unchanged to see how a single parameter influences the classification effect and computational cost. The classification accuracy and elapsed time of different parameters are shown in Figure 4.

First, we address the parameter of merging radius  $s$ , which controls the effect of adjacent point merging operation. If the distance between two points in LCS metric space is less than  $s$ , they will be merged as a local center, which means that as the value of  $s$  gets larger, there will be less point remaining after adjacent point merging. This appears at Line 9 in **Algorithm 3** in the Algorithm section, and in **Definition 7** in the paper. For classification result, we suppose that the accuracy may decrease as  $s$  getting larger because of the information loss. However, from Figure 4(a) and (b), we see that the effect of changing  $s$  differs for different dataset. In particular, the accuracy on MUTAG dataset shows a downward trend as the merging radius getting larger, but it does not change a lot on PTC-MR dataset, with two local extreme points at 0.2 and 0.4. It means that we do not always need to keep  $s$  near a great value but set it at a local extreme point where we can reduce computational cost maximally and keep a considerable accuracy meanwhile. For elapsed time, as we expected, when the merging radius gets larger, it decreases exponentially (from Figure 4(e)). At a certain point (which is near  $s = 0.2$  on PTC-MR for example), it seems that adjacent point merging operation can remove most of the repeated path sequences. If we continue to increase  $s$  after this point, the reduction of computational cost may not be so effective.

Next, we evaluate the influence of the parameter of removing ratio  $\rho$ , which means that sequences with length less than  $\rho$  percent of length of the longest sequence will be removed before

Table 3: Average classification accuracy on graphs with discrete vertex and edge labels

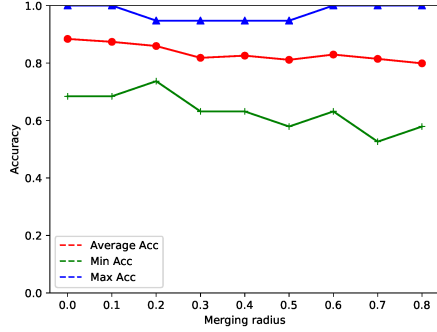
METHOD	MUTAG	PTC-FM	PTC-MR	AIDS
WLK	85.29±7.64	65.21±5.04	63.49±8.50	79.99±0.0
SPK	84.53±7.83	63.81±5.11	61.51±7.65	<b>99.58±0.42</b>
WWL	86.72±7.11	<b>68.14±7.19</b>	<b>67.01±8.34</b>	98.38±0.85
FGW	83.34±7.76	63.73±4.86	58.34±4.13	98.06±0.97
AWE	77.29±8.68	<b>67.96±6.08</b>	59.74±7.61	79.99±2.22
BLCS	<b>87.40±7.01</b>	63.89±7.06	62.53±7.01	<b>99.55±0.46</b>
FLCS	<b>88.38±7.28</b>	66.61±5.27	<b>64.50±7.24</b>	99.31±0.59

Table 4: Average classification accuracy on graphs with only discrete vertex label

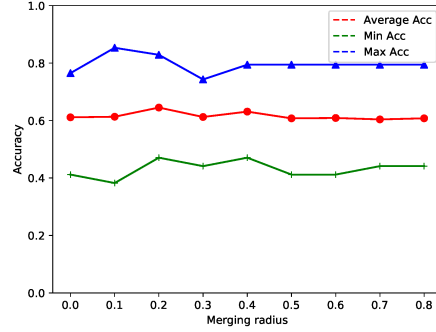
METHOD	BZR	COX2	PROTEINS	MSRC-9	MSRC-21
WLK	<b>89.14±3.25</b>	82.05±3.41	75.54±3.46	0.0±0.0	6.04±0.87
SPK	86.68±4.68	82.46±5.31	<b>76.55±3.70</b>	92.76±5.45	90.77±3.42
WWL	<b>89.54±3.87</b>	80.47±4.30	74.69±3.67	91.41±4.56	87.51±3.52
FGW	83.31±3.77	80.25±3.83	73.65±3.80	13.57±0.17	60.40±0.87
AWE	81.76±4.15	79.46±2.30	68.14±3.56	46.94±8.43	21.47±4.91
BLCS	86.70±3.72	<b>83.96±4.86</b>	<b>76.10±3.49</b>	<b>92.81±4.07</b>	<b>92.64±2.92</b>
FLCS	88.57±4.22	<b>83.01±4.18</b>	75.82±3.87	<b>93.09±3.88</b>	<b>92.64±3.10</b>

Table 5: Average classification accuracy on graphs with only discrete vertex label (including degree of node)

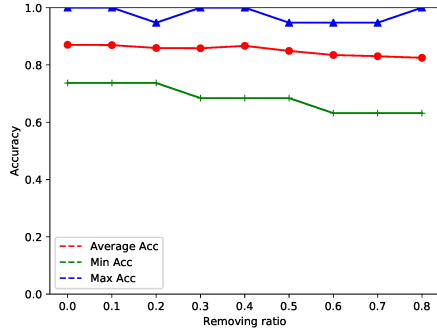
METHOD	IMDB-B	IMDB-M	MSRC-21C	ENZYMES
WLK	72.78±4.10	51.10±3.89	13.88±1.46	19.16±4.68
SPK	73.07±4.21	<b>51.71±3.97</b>	85.09±6.89	42.36±5.58
WWL	<b>73.28±3.97</b>	50.77±4.08	80.70±7.96	<b>58.46±5.94</b>
FGW	59.85±4.49	42.68±4.16	13.88±1.46	16.66±5.55
AWE	70.38±4.24	48.18±3.49	26.11±7.70	29.23±4.96
BLCS	72.52±3.94	51.29±4.35	<b>86.34±6.55</b>	<b>62.48±5.72</b>
FLCS	<b>73.30±4.33</b>	<b>51.31±4.39</b>	<b>87.16±6.43</b>	55.14±6.00



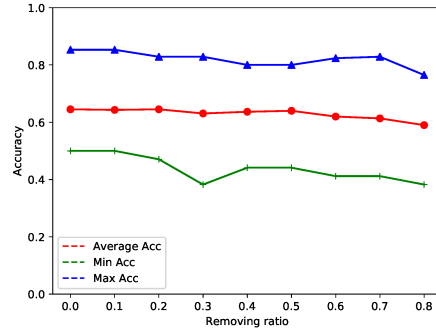
(a) Accuracy of different merging radiuses on MUTAG



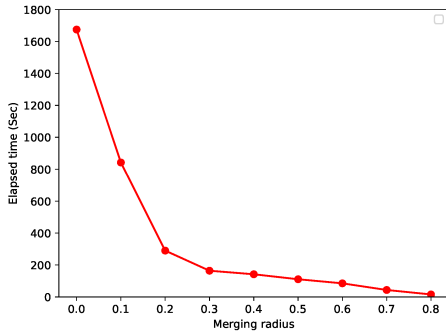
(b) Accuracy of different merging radiuses on PTC-MR



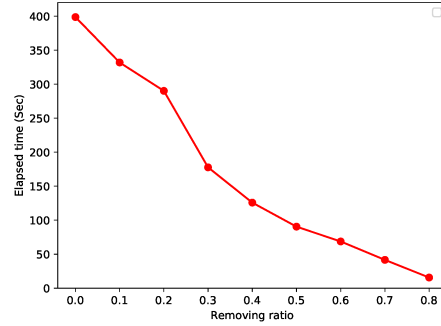
(c) Accuracy of different removing ratios on MU-TAG



(d) Accuracy of different removing ratios on PTC-MR



(e) Elapsed time of different merging radiuses on PTC-MR



(f) Elapsed time of different removing ratios on PTC-MR

Figure 4: Classification accuracy and elapsed time of the LCS kernel on MUTAG and PTC-MR. For evaluation indicator, (a), (b), (c) and (d) tests the classification accuracy; (e) and (f) tests the elapsed time of gramian matrix computing. For the parameters, (a), (b) and (e) test different merging radius  $s$  with removing ratio  $\rho$  fixed at 0.8; (c), (d) and (f) test different removing ratio  $\rho$  with merging radius  $s$  fixed at 0.8.

Table 6: Average classification accuracy on dense graph datasets

METHOD	BZR-MD	COX2-MD	ER-MD
WLK	60.78 $\pm$ 7.03	58.67 $\pm$ 8.58	67.53 $\pm$ 5.74
SPK	<b>71.12<math>\pm</math>6.69</b>	<b>66.71<math>\pm</math>9.10</b>	63.17 $\pm$ 5.96
WWL	67.43 $\pm$ 7.26	60.78 $\pm$ 7.53	69.59 $\pm$ 6.25
FGW	<b>71.03<math>\pm</math>7.48</b>	64.98 $\pm$ 7.32	<b>72.19<math>\pm</math>6.34</b>
AWE	66.90 $\pm$ 8.17	62.66 $\pm$ 7.98	68.17 $\pm$ 6.71
BLCS	70.10 $\pm$ 6.61	66.22 $\pm$ 8.14	<b>71.96<math>\pm</math>6.87</b>
FLCS	70.10 $\pm$ 6.61	<b>69.25<math>\pm</math>8.46</b>	<b>71.96<math>\pm</math>6.87</b>

Table 7: Elapsed time (Sec) for gramian matrix computing of OT-based methods

METHOD	MUTAG	COX2-MD	IMDB-B	ENZYMES
WWL	25.44	68.33	373.38	249.75
FGW	52.07	122.51	956.12	359.43
BLCS	600.19	101.68	1061.12	20191.16
FLCS	38.40	100.79	510.43	428.00

adjacent point merging operation. This also appears in at Line 4 in **Algorithm 3**. We see that the classification accuracy in Figure 4(f) shows a downward trend as the value of  $\rho$  getting larger. A too large value of  $\rho$  is not recommended, but we can still set an appropriate value like 0.2 which can keep the accuracy and reduce computational cost maximally in the meantime.

## 8 Conclusion

We have proposed a new method of computing similarity between graphs using the Wasserstein distance in LCS metric space. We present both basic and fast LCS graph kernels to perform graph classification tasks. Although LCS kernel uses only length information of LCSeq, numerical experiments reveal that it shows better performance than those of others. As future work for our research, we specifically examine more complicated information of LCSeq, such as subsequence patterns of paths, which we expect will help us to capture the key classification standard in specific classification problems. Moreover, common subsequence patterns of paths or walks are more appropriate for the input of neural networks. They can help us to build a model that includes the common feature w.r.t. a specific classification problem and which is able to embed a graph directly rather than comparing it with each graph in train data.



## References

- [1] S Vichy N Vishwanathan, Nicol N Schraudolph, Risi Kondor, and Karsten M Borgwardt. Graph kernels. The Journal of Machine Learning Research, 11:1201–1242, 2010.
- [2] Nils M Kriege, Fredrik D Johansson, and Christopher Morris. A survey on graph kernels. Applied Network Science, 5(1):1–42, 2020.
- [3] MR Gary and DS Johnson. Computers and intractability: A guide to the theory of npcompleteness wh freeman and co. New York, 1979.
- [4] N. Shervashidze, P. Schweitzer, E. J. v Leeuwen, K. Mehlhorn, and K. M. Borgwardt. Weisfeiler-lehman graph kernels. The Journal of Machine Learning Research, 12:2539–2561, 2011.
- [5] Boris Weisfeiler and Andrei A Lehman. A reduction of a graph to a canonical form and an algebra arising during this reduction. Nauchno-Tekhnicheskaya Informatsia, 2(9):12–16, 1968.
- [6] Thomas Gärtner, Peter Flach, and Stefan Wrobel. On graph kernels: Hardness results and efficient alternatives. In Learning theory and kernel machines, pages 129–143. Springer, 2003.
- [7] Karsten M Borgwardt and Hans-Peter Kriegel. Shortest-path kernels on graphs. In Fifth IEEE international conference on data mining (ICDM’05), pages 8–pp. IEEE, 2005.
- [8] C Villani. Optimal transport: Old and new. Springer, New York, 2008.
- [9] G. Peyré and M. Cuturi. Computational optimal transport. Foundations and Trends in Machine Learning, 11(5-6):355–607, 2019.
- [10] Matteo Togninalli, Elisabetta Ghisu, Felipe Llinares-López, Bastian Rieck, and Karsten Borgwardt. Wasserstein weisfeiler-lehman graph kernels. In Advances in Neural Information Processing Systems, pages 6439–6449, 2019.
- [11] David Haussler. Convolution kernels on discrete structures. Technical report, Technical report, Department of Computer Science, University of California . . . , 1999.
- [12] Robert A Wagner and Michael J Fischer. The string-to-string correction problem. Journal of the ACM (JACM), 21(1):168–173, 1974.
- [13] Thomas H Cormen, Charles E Leiserson, Ronald L Rivest, and Clifford Stein. Introduction to algorithms. MIT press, 2009.
- [14] David Maier. The complexity of some problems on subsequences and supersequences. Journal of the ACM (JACM), 25(2):322–336, 1978.
- [15] V. Seguy and M. Cuturi. Principal geodesic analysis for probability measures under the optimal transport metric. In Advances in Neural Information Processing Systems (NIPS), 2015.
- [16] Cuturi M. Rolet, A. and G. Peyré. Fast dictionary learning with a smoothed wasserstein loss. In Nineteenth International Conference on Artificial Intelligence and Statistics (AISTATS), 2016.
- [17] N. Courty, R. Flamary, and D. Tuia. Domain adaptation with regularized optimal transport. In Joint European Conference on Machine Learning and Knowledge Discovery in Databases (ECML), 2014.

- [18] M. Cuturi and A. Doucet. Fast computation of wasserstein barycenters. In Thirty-first International Conference on Machine Learning (ICML), 2014.
- [19] J. Solomon, G. Peyré, V. Kim, and S. Sra. Entropic metric alignment for correspondence problems. ACM Transactions on Graphics (TOG), 35(4):72, 2016.
- [20] R. Sinkhorn and P. Knopp. Concerning nonnegative matrices and doubly stochastic matrices. Pacific Journal of Mathematics, 21(2):343–348, 1967.
- [21] M. Cuturi. Sinkhorn distances: Lightspeed computation of optimal transport. In Annual Conference on Neural Information Processing Systems (NIPS), 2013.
- [22] J. D. Benamou, G. Carlier, M. Cuturi, L. Nenna, and G. Peyré. Iterative bregman projections for regularized transportation problems. SIAM Journal on Scientific Computing, 37(2):1111–A1138, 2015.
- [23] Hermina Petric Maretic, Mireille El Gheche, Giovanni Chierchia, and Pascal Frossard. Got: an optimal transport framework for graph comparison. In Advances in Neural Information Processing Systems, pages 13876–13887, 2019.
- [24] Vayer Titouan, Nicolas Courty, Romain Tavenard, and Rémi Flamary. Optimal transport for structured data with application on graphs. In International Conference on Machine Learning, pages 6275–6284, 2019.
- [25] Daniel Bakkelund. An lcs-based string metric. Oslo, Norway: University of Oslo, 2009.
- [26] Asim Kumar Debnath, Rosa L Lopez de Compadre, Gargi Debnath, Alan J Shusterman, and Corwin Hansch. Structure-activity relationship of mutagenic aromatic and heteroaromatic nitro compounds. correlation with molecular orbital energies and hydrophobicity. Journal of medicinal chemistry, 34(2):786–797, 1991.
- [27] Christoph Helma, Ross D. King, Stefan Kramer, and Ashwin Srinivasan. The predictive toxicology challenge 2000–2001. Bioinformatics, 17(1):107–108, 2001.
- [28] Daniel Zaharevitz. Aids antiviral screen data, 2015.
- [29] Marion Neumann, Roman Garnett, Christian Bauckhage, and Kristian Kersting. Propagation kernels: efficient graph kernels from propagated information. Machine Learning, 102(2):209–245, 2016.
- [30] Jeffrey J Sutherland, Lee A O’Brien, and Donald F Weaver. Spline-fitting with a genetic algorithm: A method for developing classification structure- activity relationships. Journal of chemical information and computer sciences, 43(6):1906–1915, 2003.
- [31] Ida Schomburg, Antje Chang, Christian Ebeling, Marion Gremse, Christian Heldt, Gregor Huhn, and Dietmar Schomburg. Brenda, the enzyme database: updates and major new developments. Nucleic acids research, 32(suppl\_1):D431–D433, 2004.
- [32] Karsten M Borgwardt, Cheng Soon Ong, Stefan Schöner, SVN Vishwanathan, Alex J Smola, and Hans-Peter Kriegel. Protein function prediction via graph kernels. Bioinformatics, 21(suppl\_1):i47–i56, 2005.

- [33] Pinar Yanardag and SVN Vishwanathan. Deep graph kernels. In Proceedings of the 21th ACM SIGKDD International Conference on Knowledge Discovery and Data Mining, pages 1365–1374, 2015.
- [34] Christopher Morris, Nils M. Kriege, Franka Bause, Kristian Kersting, Petra Mutzel, and Marion Neumann. Tudataset: A collection of benchmark datasets for learning with graphs. In ICML 2020 Workshop on Graph Representation Learning and Beyond (GRL+ 2020), 2020.
- [35] Giannis Siglidis, Giannis Nikolentzos, Stratis Limnios, Christos Giatsidis, Konstantinos Skianis, and Michalis Vazirgiannis. Grakel: A graph kernel library in python. Journal of Machine Learning Research, 21(54):1–5, 2020.
- [36] Sergey Ivanov and Evgeny Burnaev. Anonymous walk embeddings. arXiv preprint arXiv:1805.11921, 2018.